Molecular and Electronic Structure of Nitridochromium(V) Complexes with Macrocyclic Amine Ligands

Karsten Meyer, Jesper Bendix, Eckhard Bill, Thomas Weyhermüller, and Karl Wieghardt*

Max-Planck-Institut für Strahlenchemie, Stiftstrasse 34-36, D-45470 Mülheim an der Ruhr, Germany

Received March 17, 1998

Photolysis of red *cis*- and *trans*-[Cr^{III}(cyclam)$(N_3)_2$](ClO_4) (**1a**, **2a**) (cyclam = 1,4,8,11-tetraazacyclotetradecane) in the solid state or aqueous solution by light affords the nitridochromium(V) complexes of *cis*- or *trans*-[Cr^{V}(N)(cyclam)(N_3)](ClO_4) (**3a**) and dinuclear [{*trans*-[Cr^{V}(N)(cyclam)]}$_2(\mu$-$N_3)$]$(ClO_4)_3$·3.5H_2O (**4a**), respectively. **4a** was converted to the bis(tetraphenylborate)−azide−2C_2H_5OH salt (**4b**). Crystallization of **4a** from acetonitrile—after addition of $AgClO_4$ and removal of AgN_3—yields octahedral *trans*-[Cr^{V}(N)(cyclam)$(NCCH_3)$]$(ClO_4)_2$ (**5a**). The crystal structures of **1a**, **2b** (which is the tetraphenylborate salt of **2a**), **4a**,**b**, **5a**,**b** have been determined by single-crystal X-ray crystallography. All nitridochromium(V) compounds contain the *trans*-[Cr^{V}(N)(cyclam)]$^{2+}$ fragment with an N≡Cr^{V} moiety (1.56 ± 0.01 Å). The electronic spectra of d^1 configurated complexes display three low-intensity d−d bands which have been assigned in C_{4v} symmetry as (*xy*) ((*xz*,*yz*) $^2B_2 \rightarrow {}^2E$, (*xy*) → ($x^2 - y^2$) $^2B_2 \rightarrow {}^2B_1$, and (*xy*) → ($z^2$) $^2B_2 \rightarrow {}^2A_1$, where the molecular *z*-axis coincides with the N≡Cr vector. Ligand-field parameters within the angular overlap model (AOM) of $e_\sigma^{cyclam} = 7300-8600$, $e_\sigma^{ax} = 22\,000$, $e_\sigma^{ax} = 21300-25000$ cm^{-1} have been determined which reproduce the experimental electronic spectra well. Temperature-dependent magnetic susceptibility measurements and X-band EPR spectroscopy on solid samples of **4a** containing a linear Cr^{V}−N═N═N−Cr^{V} moiety revealed a weak intramolecular antiferromagnetic exchange coupling which is nearly absent in **4b** containing a bent azido bridge. A mechanism for this unexpected coupling in **4a** is proposed.

Introduction

Since the discovery that five-coordinate nitridochromium(V) complexes are synthetically readily accessible via photolysis of azidochromium(III) complexes, this class of compounds has received considerable scientific attention. The Arshankov−Poznjak reaction[1,2a] of [Cr^{III}(salen)(N_3)]·2H_2O, where salen represents the ligand *N*,*N*′-bis(salicylidene)ethylenediamine-(2−), produces [Cr^{V}(N)(salen)], a five-coordinate complex as shown in eq 1. The crystal structure of the latter has recently

$$[Cr^{III}(salen)(N_3)]\cdot 2H_2O \xrightarrow[-N_2]{h\nu} [Cr^{V}(N)(salen)]\cdot H_2O \quad (1)$$

been reported.[2b,c] While mechanisticially the photolysis reaction of $[Cr(NH_3)_5(N_3)]^{2+}$ had been studied earlier,[3,4] definitive structural proof for the formation of the Cr^{V}≡N moiety was established by X-ray crystallographically in 1983 by Groves et al.,[5] who reported the structure of [Cr^{V}(N)(ttp)] (ttp = tetratolylporphinate(2−)). This compound had been synthesized independently by hypochlorite oxidation of the chromium(III) porphyrins in the presence of NH_3.[6] Subsequently, other non-porphyrin ligands such as H_2(bpb) (1,2-bis((2-pyridylcarboxy)-amido)benzene[7] and phthalocyaninate(2− and 1−)[8] were employed. These complexes are all five-coordinate with a square-base pyramidal coordination polyhedron where the terminal nitrido ligand occupies the apical position (Table 1). The Cr≡N bond is very short at ∼1.56 Å indicative of a triple bond. A further important structural feature is the observation that the Cr^{V} ion lies ∼0.5 Å above the plane defined by the four equatorial donor atoms of the auxiliary ligand.

Recently we have published[9] the first distorted octahedral nitridochromium(V) complexes [LCr^{V}(N)(bidentate ligand)]$^{n+}$, where the bidentate ligand is oxalate, acetonyl acetate, 2-picolinate, or *o*-phenanthroline. The crystal structure of [LCr^{V}(N)(acac)](ClO_4) (L = 1,4,7-triazacyclononane) revealed that coordination of a sixth ligand in *trans*-position to the nitride weakens the Cr≡N bond (Cr−N 1.58 ± 0.01 Å). Concomitantly, the ν(Cr≡N) stretching frequency is observed at lower energy (1015 cm^{-1} in five-coordinate species and ∼967 cm^{-1} in six-coordinate species). In addition, the out-of-plane shift of the Cr^{V} ion is 0.30 Å.

The above nitridochromium(V) complexes contain a Cr^{V} ion with a d^1 electron configuration. Effective magnetic moments of 1.7−1.9 μ_B have been measured, and detailed X-band EPR investigations[5,6,10] have been reported. *For none of the above complexes have d−d transitions in their electronic spectra been identified,* and consequently, the precise electronic structure of such Cr^{V}≡N species is largely unknown. Since this is due to the fact that all auxiliary ligands employed so far display intense charge-transfer bands in the region where these weak d−d transitions might be expected, we decided to synthesize a series of complexes containing spectroscopically "innocent" ligands.

(1) Arshankov, S. I.; Poznjak, A. L. *Z. Anorg. Allg. Chem.* **1981**, *481*, 201.
(2) (a) Arshankov, S. I.; Poznjak, A. L. *Russ. J. Inorg. Chem.* **1981**, *26*, 850. (b) Azuma, N.; Imori, Y.; Yoshida, H.; Tajima, K.; Li, Y.; Yamauchi, J. *Inorg. Chim. Acta* **1997**, *266*, 29. (c) Bendix, J.; Wilson, S. R.; Prussak-Wiechowska, T. *Acta Crystallogr.* **1998**, *C54*, 923.
(3) Sriram, R.; Endicott, J. F. *Inorg. Chem.* **1977**, *16*, 2766.
(4) Katz, M.; Gafney, H. D. *Inorg. Chem.* **1978**, *17*, 93.
(5) Groves, J. T.; Takahashi, T.; Butler, W. M. *Inorg. Chem.* **1983**, *22*, 884.
(6) Buchler, J. W.; Dreher, C.; Lay, K.-L.; Raap, A.; Gersonde, K. *Inorg. Chem.* **1983**, *22*, 879.
(7) Che, C.-M.; Ma, J.-X.; Wong, W.-T.; Lai, T.-F.; Poon, C.-K. *Inorg. Chem.* **1988**, *27*, 2547.
(8) Grunewald, H.; Homborg, H. *Z. Anorg. Allg. Chem.* **1992**, *608*, 81.
(9) Niemann, A.; Bossek, U.; Haselhorst, G.; Wieghardt, K.; Nuber, B. *Inorg. Chem.* **1996**, *35*, 906.
(10) Azuma, N.; Ozawa, T.; Tsuboyama, S. *J. Chem. Soc., Dalton Trans.* **1994**, 2609.

S0020-1669(98)00302-4 CCC: $15.00
Published on Web 09/16/1998

Table 1. Comparison of Structural Data for X-ray Crystallographically Characterized Nitridochromium(V) Complexes

complex	CN	*d*(Cr≡N), Å	*d*(out-of-plane), Å	ref
[Cr(N)(salen)]	5	1.544(3)	0.499(3)	2b
[Cr(N)(ttp)]	5	1.565(6)	0.42	5
[Cr(N)(bpb)]	5	1.560(2)	0.51	7
[LCr(N)(acac)](ClO_4)	6	1.575(9)	0.30	9

Chart 1. Complexes Prepared and Labels

cis-[Cr^{III}(cyclam)(N_3)$_2$](ClO_4) **1a**

trans-[Cr^{III}(cyclam)(N_3)$_2$]X X = ClO_4 **2a**

BPh_4 **2b**

trans-[Cr^{V}(N)(cyclam)(N_3)]X X = ClO_4 **3a**

BPh_4 **3b**

[{*trans*-[Cr^{V}(N)(cyclam)]}$_2$ (μ-N_3)](ClO_4)$_3$ • 3.5 H_2O **4a**

[{*trans*-[Cr^{V}(N)(cyclam)]}$_2$ (μ-N_3)](BPh_4)$_2$(N_3) • 2 C_2H_5OH **4b**

trans-[Cr^{V}(N)(cyclam)($NCCH_3$)]X_2 X = ClO_4 **5a**

BPh_4 **5b**

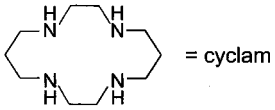

We report here on [Cr^{V}(N)(cyclam)Y]$^{n+}$ complexes (Chart 1) for which we have unambiguously detected and assigned three d−d transitions (cyclam = 1,4,8,11-tetraazacyclotetradecane).

Results and Discussion

Preparation of Complexes. Complexes prepared in this work and their labels are shown in Chart 1.

From the reaction mixture of *cis*-[Cr^{III}(cyclam)Cl_2]Cl[11] and an excess NaN_3 in ethanol under reflux an insoluble microcrystalline red precipitate of *cis*-[Cr^{III}(cyclam)(N_3)$_2$](N_3) was obtained in ∼50% yield.[11b] From the filtered, deep red solution red crystals of *trans*-[Cr^{III}(cyclam)(N_3)$_2$]X (X = ClO_4^- (**2a**), BPh_4^- (**2b**)) were obtained in similar yields upon addition of $NaClO_4$ or $NaBPh_4$. *cis*-[Cr^{III}(cyclam)(N_3)$_2$](N_3) was converted to the corresponding perchlorate salt (**1a**) from an acetonitrile/water mixture (5:1) by addition of 0.10 M $HClO_4$. Complexes **1a** and **2a**,**b** are light sensitive both in solution and in the solid state and must be stored in the dark.

Figure 1 displays the electronic spectra of **1a** and **2a** in aqueous solution. In approximate O_h symmetry the two d−d transitions in the visible are assigned $^4A_{2g} \rightarrow {}^4T_{2g}$(F) and $^4A_{2g} \rightarrow {}^4T_{1g}$(F) from which the ligand field splitting energy 10*Dq* is calculated to be 19 010 cm^{-1} for **1a** and 18 760 cm^{-1} for **2a**. Traditionally, the Racah parameter *B* is estimated from the strong-field approximations given in eqs 2 and 3. This gives

$$\Delta E_1 = ({}^4T_{2g}(F) - {}^4A_{2g}) = 10Dq \quad (2)$$

$$\Delta E_2 = ({}^4T_{1g}(F) - {}^4A_{2g}) = 10Dq + 12B \quad (3)$$

the values 466 cm^{-1} for **1a** and 641 cm^{-1} for **2a**. If interaction between $^4T_{1g}$(F) and the unobserved $^4T_{1g}$(P) is taken into account, *B* values of 520 cm^{-1} (**1a**) and 776 cm^{-1} (**2a**) are determined. The difference between the *B* values determined by the two methods is a measure of the departure from the limiting strong-field coupling scheme, which is moderate for these systems. For *cis*- and *trans*-[Cr^{III}(cyclam)Cl_2]$^+$ values for 10*Dq* and *B* have been determined by use of the full d^3 matrixes as 18870/17640 and 549/744 cm^{-1}, respectively.[11]

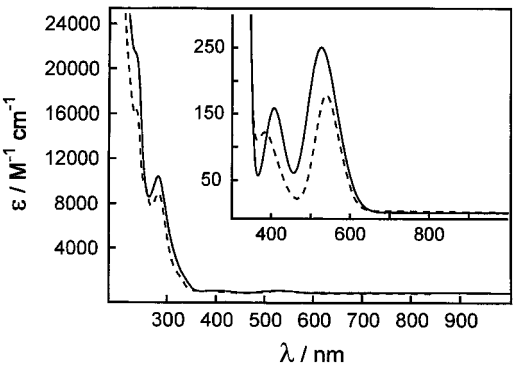

Figure 1. Electronic spectra of **1a** (—) and **2a** (- - -) in H_2O. The inset shows the visible region of the spectra.

When small red, rod-shaped crystals of **2b** were exposed to normal daylight, a color change from red to bright yellow was observed within a few hours and *trans*-[Cr^{V}(N)(cyclam)(N_3)](BPh_4) (**3b**) was obtained in quantitative yield. On a preparative scale we have illuminated on aluminum foil thinly dispersed crystalline materials of **1a** and **2a**,**b** with a 300 W light bulb. During this illumination a color change from red to yellow was observed and, concomitantly, a loss of weight of the solid materials due to the evolution of dinitrogen. The reaction was usually complete within 4 h; only in the case of **1a** ∼20% of the starting material did not react. Therefore, we did not further characterize *cis*-[Cr^{V}(N)(cyclam)(N_3)]X complexes. It was established manometrically and gravimetrically that 1.0 ± 0.1 equiv of N_2/chromium(III) center evolved from **2a**,**b**, respectively, with generation of the nitridochromium(V) species **3a**,**b**. The formation of a Cr^{V}≡N group in **3a**,**b** was detected in the infrared spectra of yellow samples where a new band at 973 cm^{-1} is assigned to the ν(Cr≡^{14}N) stretching mode. This was proven by using $^{15}N-{}^{14}N^{14}N$ labeled **2a**. Upon irradiation of such a sample *two* new bands at 973 and 950 cm^{-1} of equal intensity are indicative of the (Cr≡^{14}N) and (Cr≡^{15}N) isotopomers of *trans*-[Cr^{V}(N)(cyclam)(N_3)](ClO_4) (**3a**).

Attempts to recrystallize **3a** from aqueous solutions resulted in the quantitative formation of the yellow dinuclear species [{*trans*-[Cr^{V}(N)(cyclam)]}$_2$(μ-N_3)](ClO_4)$_3$·3.5H_2O (**4a**). This complex was also obtained when aqueous solutions of **2a** or **1a** at ambient temperature were photolyzed by using a Hg immersion lamp. The amount of N_2 measured manometrically showed that again 1 equiv of N_2/chromium(III) ion is generated forming the [Cr^{V}(N)(cyclam)]$^{2+}$ fragment. The salt [{*trans*-[Cr^{V}(N)(cyclam)]}$_2$(μ-N_3)](BPh_4)$_2$(N_3)·2C_2H_5OH (**4b**) was obtained from an ethanol/acetone (1:1) mixture of **3b**.

Crystallization of **4a**,**b** from acetonitrile solutions to which 1 or 2 equiv of $AgClO_4$, respectively, had been added and from which AgN_3 had been removed by filtration yielded bright yellow crystals of *trans*-[Cr^{V}(N)(cyclam)($NCCH_3$)]X_2, where X is ClO_4^- (**5a**) or BPh_4^- (**5b**). In the infrared spectra the ν(Cr≡N) stretch has been identified at 995 and 998 cm^{-1}, respectively.

Crystal Structures. The structures of complexes **1a**, **2b**, **4a**,**b**, and **5a**,**b** have been determined by X-ray crystallography. A summary of structural parameters is given in Table 2.

Figure 2 shows the structures of the *cis*- and *trans*-[Cr^{III}(cyclam)(N_3)$_2$]$^+$ cations in crystals of **1a** and **2b**. The chro-

(11) (a) Poon, C. K.; Pun, K. C. *Inorg. Chem.* **1980**, *19*, 568. (b) Ferguson, J.; Tobe, M. L. *Inorg. Chim. Acta* **1970**, *4*, 109.

Table 2. Summary of Selected Bond Distances (Å) and Angles (deg) for **1a**, **2b**, **4a**,**b**, and **5a**,**b**

	complex					
	1a	**2b**	**4a**	**4b**	**5a**	**5b**
Cr−N1	2.103(3)	2.059(4)	2.049(4)	2.049(3)	2.074(3)	2.054(3)
Cr−N2	2.069(3)	2.052(4)	2.042(4)	2.081(3)	2.061(3)	2.073(3)
Cr−N3	2.100(3)	2.073(4)	2.055(4)	2.084(3)	2.058(3)	2.070(3)
Cr−N4	2.092(3)	2.063(3)	2.073(4)	2.050(3)	2.075(3)	2.037(3)
Cr−N5	1.996(3)	2.030(4)		1.557(3)	1.561(3)	1.545(2)
Cr−N6				2.350(3)	2.432(3)	2.418(3)
Cr−N8	2.028(3)	1.924(4)				
Cr−N9			1.559(4)			
Cr−N20			2.322(5)			
N5−N6	1.187(4)	1.205(6)				
N6−N7	1.143(4)	1.180(6)	1.133(5)	1.180(3)		
N8−N9	1.120(4)	1.211(6)				
N9−N10	1.163(4)	1.184(6)				
av N_5-Cr-N_5[a]	82.7(1)	85.6(2)	84.5(2)	84.5(1)	84.6(1)	84.9(1)
av N_6-Cr-N_6[b]	88.8(1)	94.4(1)	93.6(2)	93.9(1)	93.5(1)	93.3(1)
θ[c]			97.1(2)	96.8(2)	97.4(2)	97.3(2)

[a] Average $N_{amine}-Cr-N_{amine}$ bond angle of the two five-membered (cyclam)Cr chelate rings. [b] Average $N_{amine}-Cr-N_{amine}$ bond angle of the two six-membered (cyclam)Cr chelate rings. [c] Average N≡Cr−N_{amine} bond angle.

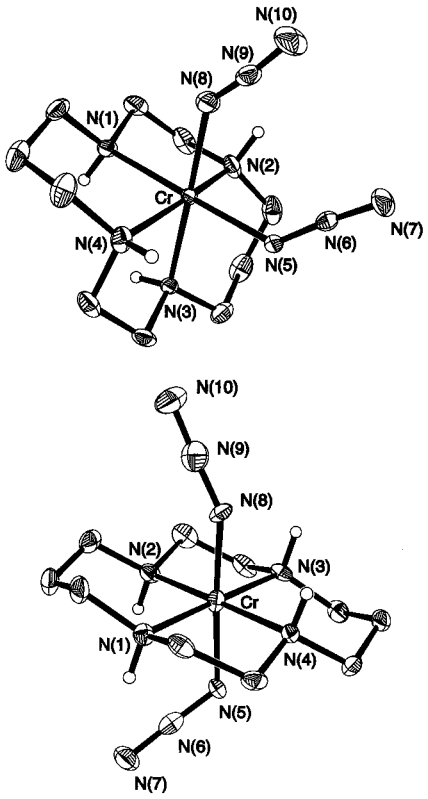

Figure 2. Perspective views of the monocations in crystals of **1a** (top) and **2b** (bottom).

mium(III) ion in **2b** is in a nearly perfect octahedral N_6 environment comprising four equatorial amine nitrogen donors and two axial azide N-donors. The amine nitrogens lie in a plane (average deviation ± 0.0005 Å) with the Cr^{III} ion in its center (Δd = 0.0002 Å). The ligand cyclam is coordinated in its energetically most favorable *trans*-III configuration[12] having the least ring strain. The absolute configuration at the nitrogen atoms is *RRSS*. According to the differing chelate ring size the N−Cr−N bond angles are ∼5° smaller in the five-membered Cr−N−C−C−N rings and ∼5° larger in the corresponding six-membered rings than the ideal octahedral angle of 90°. The Cr−N_{cyclam} bonds are within the 3σ limits equidistant at 2.06 ± 0.01 Å. In contrast, the two azido ligands in *trans*-position relative to each other are not equivalent: Cr−N5 is longer at 2.030(4) Å than Cr−N8 at 1.924(4) Å and, also, the Cr−N_α−N_β bond angles are significantly different at 123.2(3) and 147.8(4)°, respectively. This indicates that one N_3^- ligand is slightly more covalently bound (N8−N9−N10) to Cr^{III} than the other one (N5−N6−N7).

In crystals of **1a** the cation *cis*-$[Cr^{III}(cyclam)(N_3)_2]^+$ is present where the chromium(III) is also in an octahedral environment of six nitrogens. The ligand cyclam adopts a *cis*-configuration,[12] and consequently, the two coordinated azide ligands are in *cis*-position relative to each other. The two Cr−N_{amine} bond distances in *trans*-position relative to the azide ligands are equidistant at 2.100(3) and 2.103(3) Å. They are slightly longer than the other two Cr−N_{amine} bonds at 2.08 ± 0.01 Å. The Cr−N_{azide} bonds are again slightly different at 1.996(3) and 2.028(3) Å as are the corresponding Cr−N_α−N_β bond angles at 130.9(2) and 138.0(3)°, respectively.

Crystals of **4a**,**b** and **5a**,**b** consist of cations containing the *trans*-$[Cr^V(N)(cyclam)]^{2+}$ fragment, the structural parameters of which are very similar regardless of the nature of the sixth coordinated ligand which is a bridging azide in **4a**,**b** and an acetonitrile ligand in **5a**,**b**. Interestingly, the coordinated cyclam ligand adopts the same *trans*-III configuration as in *trans*-$[Cr^{III}(cyclam)(N_3)_2]^+$ (**2b**). Even the Cr^V−N_{amine} bond distances at 2.06 ± 0.01 Å are the same as in **2b**. Thus there is no shortening of these bonds on going from a Cr^{III} to a high-valent Cr^V central ion. The Cr≡N bond is in all cases very short at 1.56 ± 0.01 Å indicating a genuine triple bond. The average N≡Cr−N_{amine} bond angle, θ, is significantly larger at ∼97.2° than the ideal octahedral angle of 90°, and consequently, the Cr^V ion lies 0.25 Å above the plane defined by the four amine nitrogen atoms. In **2b** the Cr^{III} ion lies in this plane (θ = 90°), but in five-coordinate N≡Cr^V species θ is even larger and the Cr^V ion is displaced up to ∼0.5 Å from the equatorial plane (Table 1).

The dinuclear trications in crystals of **4a**,**b** consist of two *trans*-$[Cr^V(N)(cyclam)]^{2+}$ fragments bridged in an end-to-end 1,3-fashion by one azide (Figure 3) rendering the Cr^V ions six-coordinate. The Cr^V−N_{azide} bonds are in *trans*-position relative to the N≡Cr bond which exerts a pronounced *trans*-influence on the Cr^V−N_{azide} bond. This bond distance is longer by 0.26 Å in **4a** and by 0.29 Å in **4b** than the average Cr^V−N_{amine} bond. Note that in **2b** the Cr^{III}−N_{azide} bonds are *shorter* than the Cr^{III}−N_{amine} bonds.

Due to crystal packing effects the conformation of the trication in **4a** differs from that in **4b**. In **4a** the N≡Cr−N−N−N−Cr≡N unit is nearly linear; the Cr^V−N_α−N_β bond angle is 172.6(5)°, the N≡Cr−N_α angle is 176.1°, and the N_α−N_β−N_γ angle is 179.3(9)°. The trication is bisected by crystallographic mirror plane (C_s symmetry), and N7 lies on this plane; consequently, the two coordinated cyclam ligands are eclipsed. In contrast, the same trication in crystals of **4b** has crystallographically imposed C_i symmetry, where N7 lies on an inversion center. The Cr^V−N_α−N_β angle is now only 141.7(1)°, whereas the N≡Cr−N_α angle is 176.9(2)° and N6−N7−N6a is 180.0°.

A closer inspection of the packing in **4a** reveals that each trication forms an ion pair with two ClO_4^- anions, $\{[\{(cyclam)Cr(N)\}_2(\mu\text{-}N_3)](ClO_4)_2\}^+$, via four intramolecular N_{cyclam}−H··· O_{ClO_4} contacts (two to each coordinated cyclam). The third disordered ClO_4 anion is not involved in hydrogen bonding.

(12) (a) Bosnich, B.; Poon, C. K.; Tobe, M. L. *Inorg. Chem.* **1965**, *4*, 1102. (b) Adam, K. R.; Atkinson, I. M.; Lindoy, L. F. *Inorg. Chem.* **1997**, *36*, 480.

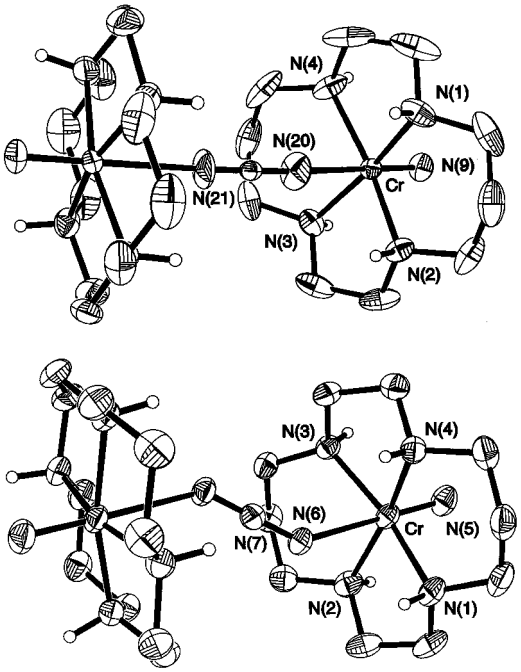

Figure 3. Perspective views of the trications in crystals of **4a** (top) and **4b** (bottom) emphasizing the nearly linear N≡Cr−N=N=N−Cr≡N moiety in **4a** and bent in **4b**.

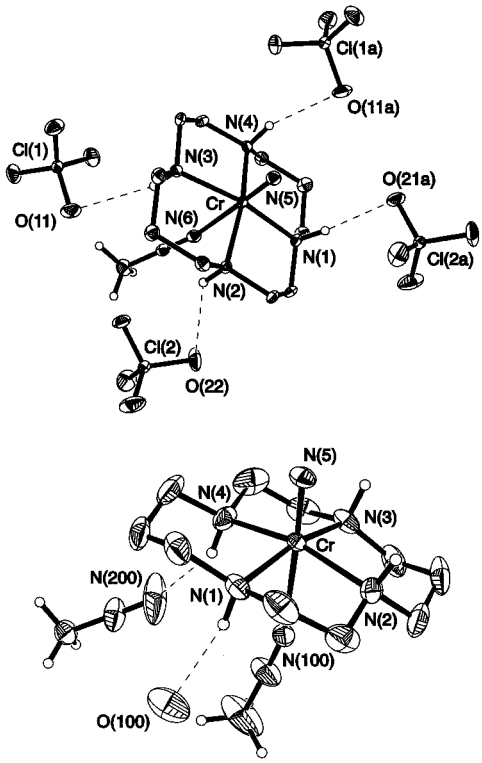

Figure 4. Perspective views of the dications in crystals of **5a** (top) and **5b** (bottom) showing the O···H−N and N···H−N hydrogen-bonding contacts to the amine hydrogens and ClO_4^- and the CH_3CN and H_2O molecules of crystallization, respectively.

Similarly, in **4b** the anionic (not coordinated) azide forms two intramolecular $N_{cyclam}-H\cdots N_{azide}$ hydrogen bonds and two $O_{C_2H_5OH}-H\cdots N_{azide}$ contacts where these two ethanol molecules form two $N_{cyclam}-H\cdots O_{C_2H_5OH}$ bonds yielding the dicationic ion pair $\{[\{(cyclam)Cr(N)\}_2(\mu\text{-}N_3)]N_3\cdot 2(C_2H_5OH)\}^{2+}$. The two tetraphenylborate anions are well separated from these dicationic ion pairs. The formation of these differing ion pairs in **4a**,**b** shown in Chart 2 may be the origin of the above conformational differences of the bridging azide observed.

Chart 2. Ion Pairing in Crystals of **4a** and **4b**

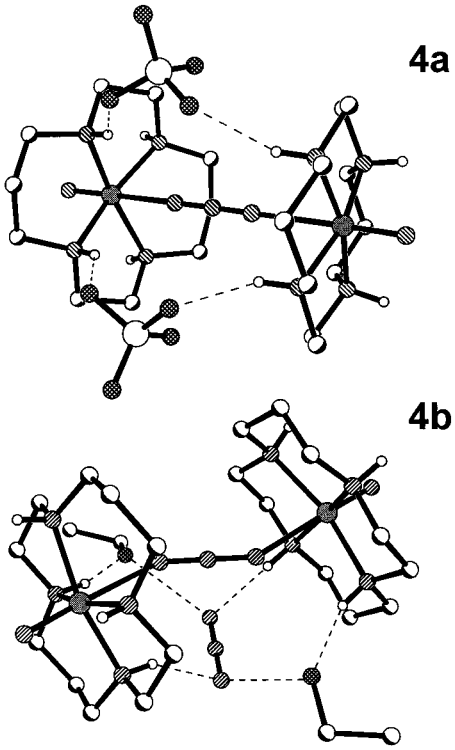

In crystals of **5a**,**b** the six-coordinate dication *trans*-$[Cr^V(N)(cyclam)(NCCH_3)]^{2+}$ is present (Figure 4) as well as perchlorate anions in **5a** and tetraphenylborate anions and uncoordinated acetonitrile and water molecules of crystallization in **5b**. In both structures the nitridochromium(V) bond is short at 1.55 ± 0.01 Å and exerts a strong *trans*-influence on the $Cr-N_{CH_3CN}$ bond in the *trans*-position. This bond at 2.43 ± 0.01 Å is rather long.

In **5a** the perchlorate anions form a weak hydrogen bond to the amine hydrogens. Therefore, these anions are not disordered ($O_{ClO_4}\cdots N_{cyclam}$ 3.0−3.2 Å). In **5b** the uncoordinated CH_3CN forms a weak hydrogen bonding contact to an amine nitrogen (N7···H−N4) and the water molecule is hydrogen bonded to N1 (O···H−N).

Magnetism. We have measured the magnetic susceptibilities of solid samples of complexes in the temperature range 4.2−300 K in an 1.0 or 0.10 T magnetic field by using a SQUID magnetometer. The observed molar susceptibilities were corrected for both underlying diamagnetism by use of Pascal's tabulated constants and, in the case of Cr^V species, for temperature-independent paramagnetism, (150−190) × 10^{-6} cm^3 mol^{-1} per Cr^V ion.

In excellent agreement with the d^3 electron configuration of the chromium(III) ions in **1a** and **2a** temperature-independent (30−300 K) magnetic moments of 3.85 and 3.77 μ_B, respectively, have been observed. The mononuclear species **3b** and **5a** display in the temperature range 10−300 K a fully temperature-independent magnetic moment of 1.71 ± 0.01 μ_B. Consequently, the plot $\chi_M T$ vs T for **3b** shown in Figure 5 yields a straight line. From these susceptibility measurements g values of 1.971 for **3b** and 1.988 for **5a** have been calculated in good agreement with values determined by EPR spectroscopy (see below). These magnetic moments represent the expected spin-

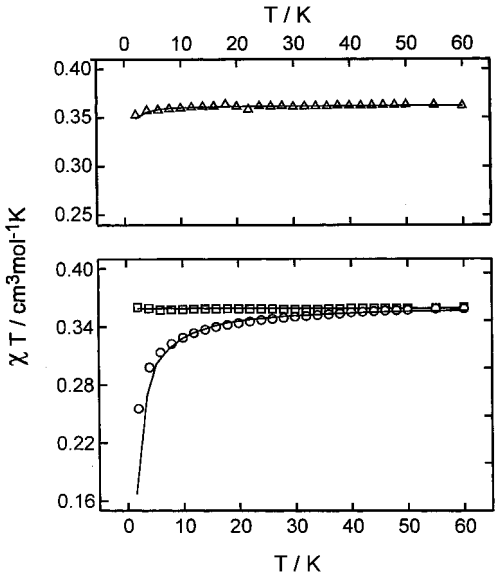

Figure 5. Plot of $\chi_M T$ versus T for complexes **4b** (△) (top) and **3b** (□) and **4a** (○) (bottom). Note that the χ_M values for **4a**,**b** are calculated per chromium(V) ion for the sake of comparability with the mononuclear species. The solid lines represent fits described in the text. The experimental susceptibility data were measured in an applied field of 0.10 T.

only values for a d^1 electron configuration with quenching of the orbital contributions to the magnetic moment.

The magnetic properties of the dinuclear species **4a**,**b** are interesting because both contain two d^1 configurated Cr^V ions bridged by an azide ion where the only significantly differing structural parameter is the $Cr-N_\alpha-N_\beta$ bond angle (see above). Figure 5 displays the plots of $\chi_M T$ vs T for **4a** containing a linearly bridged dication and for **4b** which has the bent structure. Clearly, in the temperature range 4−80 K $\chi_M T$ for **4a** decreases somewhat with decreasing temperature which it does much less so for **4b**. At temperatures >80 K both species exhibit a temperature-independent magnetic moment of $1.71 \pm 0.01\ \mu_B$ per Cr^V ion. This behavior is typical for a weakly antiferromagnetically coupled system in **4a** and nearly uncoupled behavior in **4b**. Together with the EPR results presented below for **4a** it is clear that the observed weak antiferromagnetic coupling in solid **4a** is intra- rather than intermolecular in nature. A fit of the data using the usual spin-Hamiltonian $H = -2J(S_1 \cdot S_2)$ ($S_1 = S_2 = {}^1/_2$) affords a coupling constant, J, of $-1.2\ cm^{-1}$ for **4a** using a g value of 1.969 from the EPR measurements. In contrast, for **4b** a J value of $-0.1\ cm^{-1}$ and $g = 1.983$ was obtained. This coupling is very small indeed and may be at the detection limit of bulk magnetic susceptibility measurement. Thus **4b** may lack a coupling altogether.

EPR Spectroscopy. X-band EPR spectra of **5a** have been measured at low (30 K) and ambient temperature (290 K) both in the solid state and in CD_3CN solution. Figure 6 shows the solution spectra at 30 and 290 K and the respective simulation. The room-temperature spectrum displays an isotropic signal at $g_{iso} = 1.9865$ with a relatively small line width of ∼2 mT which allows the detection of a resolved hyperfine structure due to coupling of the unpaired electron with the nuclear spin of the less abundant ^{53}Cr isotope (9.5% ^{53}Cr; $I = {}^3/_2$). A coupling constant, $A_{iso}(^{53}Cr)$, of 2.7 mT was obtained from the simulation. The spectrum of a frozen CD_3CN solution at 30 K shows the expected axial signal with $g_\perp = 1.997$ and $g_\parallel = 1.965$ ($g_\perp > g_\parallel$ for d^n systems with $n < 5$). From the relation $\langle g\rangle^2 = {}^1/_3(2g_\perp{}^2 + g_\parallel{}^2)$ an average $\langle g\rangle$ value of 1.986 is calculated which is identical with the observed g-value at 290 K. Simulation of this spectrum gave $A_\perp(^{53}Cr) = 1.6$ mT and $A_\parallel(^{53}Cr) = 4.2$ mT in excellent agreement with $A_{iso} = \langle A\rangle = 2.7$ mT. Similar values have been reported for $[Cr^V(N)(bpb)]$,[10] $[Cr^V(N)(oep)]$,[6] and $[Cr^V(N)(ttp)]$,[6] where H_2bpb represents 1,2-bis((2-pyridylcarboxy)amido)benzene, oep = octaethylporphinate(2−), and ttp = tetratolylporphinate(2−) (see Table 3).

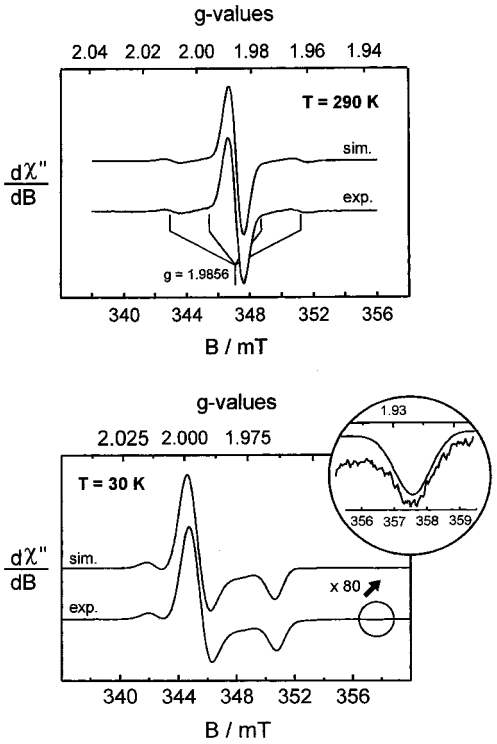

Figure 6. X-band EPR spectra of **5a** in CD_3CN at 290 K (top) and 30 K (bottom). Experimental conditions: at 290 K, microwave frequency 9.6461 GHz, microwave power 2.0 mW, modulation amplitude 14.4 μT; at 30 K, 9.6448 GHz, 100 μW, 0.57 mT, respectively. The simulations were performed (290 K, $W = 2$ mT; 30 K, $W_\perp = 1.8$ mT, $W_\parallel = 1.5$ mT) with parameters given in the text and Table 3.

Table 3. Summary of EPR Spectroscopic Parameters of Nitridochromium(V) Complexes

	complex					
param	**3b**	**4a**	**4b**	**5a**	[Cr(N)-(bpb)][a]	[Cr(N)(oep)],[b] [Cr(N)(ttp)]
g_{iso}	1.983	1.969(∼4)	1.983	1.9856	1.9830	1.9825
$A(^{53}Cr)$, mT				2.80	2.84	2.83
$A(^{14}N)$, mT				0.23	0.23	0.27
$g_\perp$				1.997	1.992	1.9945
$g_\parallel$				1.965	1.956	1.9583
$\langle g\rangle$[c]				1.986	1.980	1.9824
$A_\perp(^{53}Cr)$, mT				1.60	2.21	2.24
$A_\parallel(^{53}Cr)$, mT				4.20	4.41	4.01
$\langle A\rangle$, mT[d]				2.75	2.94	2.83

[a] Reference 6. [b] Reference 7. [c] Calculated value using $\langle g\rangle^2 = {}^1/_3(2g_\perp{}^2 + g_\parallel{}^2)$. [d] Calculated value using $\langle A\rangle^2 = {}^1/_3(2A_\perp{}^2 + A_\parallel{}^2)$.

In the EPR spectra of $[Cr^V(N)(oep)]$, $[Cr^V(N)(ttp)]$, and $[Cr^V(N)(bpb)]$ additional signals due to hyperfine interactions with ^{14}N nuclei ($I = 1$) are reported.[6,10] In contrast to the pyrrol nitrogens in oep and ttp the amine nitrogens of the ligand cyclam in **5a** carry a bound hydrogen with a nuclear spin of $^1/_2$ which gives rise to a super-super hyperfine interaction. Thus 9 of the expected 13 signals of an Cr^VN_6 octahedron are split into doublets. Even using very small modulation amplitudes these interactions cannot be resolved in X-band, and consequently, only the envelope of signals was observed for **5a** under the above experimental conditions. Addition of *one drop* of D_2O

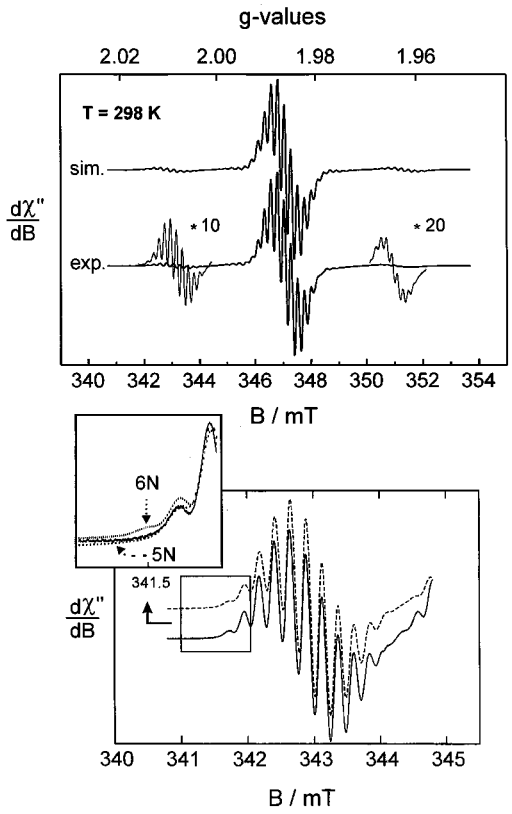

Figure 7. Top: X-band EPR spectrum of *trans*-[Cr^{V}(N)(d_4-cyclam)($NCCD_3$)](ClO_4)$_2$ (**5a**) in CD_3CN/D_2O (9:1) at 298 K. Experimental conditions: microwave frequency 9.64742 GHz; microwave power 2.0 mW, modulation amplitude 14.4 μT. Experimental spectrum (—) of the low-field signal at ~343 mT and its simulation (- - -). The inset shows the simulated effect of 5 versus 6 nitrogen donor atoms on the hyperfine splitting pattern.

(~10 μL) to the above CD_3CN solution of **5a** affects a deuterium exchange of the amine protons. Since $A_{iso}(^2H)$ is $\sim^1/_7$ $A_{iso}(^1H)$, this H → D exchange should make the electron−nitrogen nuclei coupling visible. The experimental result shown in Figure 7 demonstrates that this is indeed the case. A superhyperfine coupling constant of $A_{iso}(^{14}N) = 0.23$ mT is established.

From a simulation of the low-field signal ($m_I = -^3/_2$) shown in Figure 7 (bottom) it has been possible to establish that only 5 nitrogens carry spin density. The weakly bound acetonitrile nitrogen of the dication **5a** is not involved. The 5 equivalent nitrogens give rise to an intensity distribution of 1:5:15:30:45:51:45:30:15:5:1, whereas 6 nitrogens give 1:6:21:50:90:126:141:126.... Thus the intensity ratio of the weakest signals to the most prominent central signal is 1:50 or 1:140.

The X-band EPR spectrum of **3b** in CH_3CN at 30 K displays a broad isotropic signal at $g_{iso} = 1.983$. This spectrum is very similar to that of **4b** measured under the same conditions and gives also $g_{iso} = 1.983$.

Figure 8 shows the X-band EPR spectrum of **4a** in the solid state at 10 K which displays a prominent isotropic signal at $g_{iso} = 1.969$. Interestingly, at about 10-fold increased microwave power an additional weak signal at $g \sim 4$ is observed. This signal at half-field is typical of the "forbidden" $\Delta m_s = 2$ transition ($m_s = -1$ to $m_s = +1$) in a spin triplet ($S = 1$) that results from spin coupling. The transitions gain intensity by mixing of $m_s = \pm 1$ with $m_s = 0$ states due to zero-field splitting of the triplet levels caused by dipolar coupling. We mention that the widths of the allowed transitions are about 10 times the widths of the Cr^{V} monomers, which also reflects the nonresolved zero-field splittings of the coupled system. The

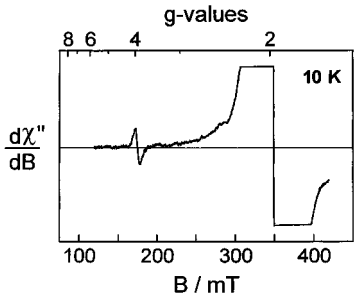

Figure 8. X-band EPR spectrum of solid **4a** at 10 K. Experimental conditions: microwave frequency 9.6548 GHz, microwave power 100 μW, modulation amplitude 0.51 mT.

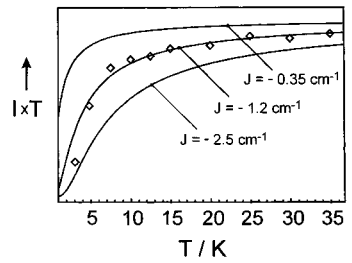

Figure 9. Plot of the product intensity × temperature, *IT*, versus *T* of the $g \sim 2$ signal of **4a**. The solid lines represent fits to eq 4.

triplet state must be due to an intramolecular exchange interaction between the two Cr^{V} ions ($S = ^1/_2$). We have recorded a series of such EPR spectra in the temperature range 2−35 K using extremely small microwave power of 200×10^{-9} W and found that the intensity of the $g \sim 2$ signal decreases with decreasing temperature due to the fact that a diamagnetic $S = 0$ ground state is populated and the excited, EPR-active $S = 1$ state is depopulated. Using the Boltzmann function in eq 4,

$$IT = \text{const}\cdot(\exp(-2|J|/kT))/(1 + 3\exp(-2|J|/kT)) \quad (4)$$

the best fit of the data yielded a coupling constant J of -1.2 cm^{-1} in excellent agreement with the bulk magnetic susceptibility measurements of **4a**. The fit is shown in Figure 9; it is very sensitive to small variations of J. Thus a value of -2.5 or -0.35 cm^{-1} does not give a satisfactory fit.

Interestingly, for **4b** in the solid state at 10 K the $g \sim 4$ signal has not been detected and the solution spectra of **4a**,**b** in CH_3CN also lack this signal. We take this as an indication that **4b** in the solid state exhibits only an extremely weak intramolecular antiferromagnetic coupling—if any at all.

In the following we attempt to rationalize the differing magnetic behavior of **4a**,**b** within the frame of the Good-enough−Kanomori rules for superexchange. The unpaired electrons in both cations are in d_{xy} metal orbitals where the N≡Cr vector defines the *z*-axis and the $Cr-N_{cyclam}$ bonds roughly coincide with the *x*- and *y*-axes. Chart 3 clearly shows that the possible π-exchange pathways involving a linear azide bridge lead to ferromagnetic interactions since the $d_{xy}|p_x|d_{xy}$ and $d_{xy}|p_y|d_{xy}$ interactions are orthogonal (A). The $\delta-\pi$ interaction $d_{xy}|p_z|d_{xy}$ (C) yields also a ferromagnetic contribution. Only the σ-pathway $d_{z^2}|p_z|d_{z^2}$ (B) would result in an antiferromagnetic contribution if spin density is present in the d_{z^2} orbital. This could be achieved by mixing of the singly occupied d_{xy} with the empty d_{z^2} orbital upon reduction of the symmetry from C_{4v} to C_s. An indication that this might be the case comes from the observation that the $g_{||}$ values in the EPR spectra of **5a** and [Cr(N)(ttp)][6] are shifted to higher fields (Table 3). This antiferromagnetic σ-exchange pathway B is then considerably

Chart 3. Orbital Interactions.

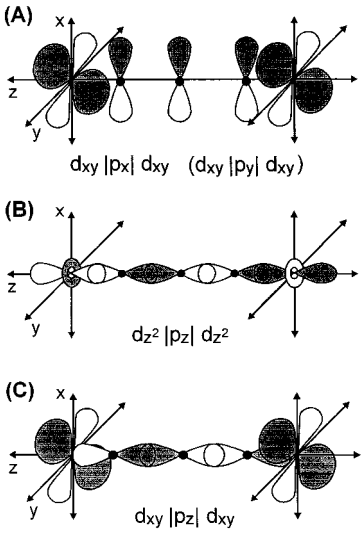

Table 4. Electronic Spectral Data for Nitridochromium(V) Complexes in Acetonitrile Solution

	λ_{max}, nm (ϵ, L mol^{-1} cm^{-1})				
complex	I ($^2B_2 \rightarrow {}^2E$)[a]	II ($^2B_2 \rightarrow {}^2B_1$)[a]	III ($^2B_2 \rightarrow {}^2A_1$)[a]	$N_3^- \rightarrow Cr$ LMCT	N_3^- ($\pi-\pi^*$)
3b	440 sh (30)	404 (55)	365 (60)	310 sh (440)	273 sh (3070)
4a	427 (45)	396 (90)	363 (66)	310 sh (600)	255 (4000)
5a	435 (16)	399 (50)	342 (25)		
5b	430 sh (30)	397 (65)	335 (35)		

[a] The band positions, λ_{max}, given are the result of a fit using three absorption maxima of Gaussian line shape; the absorption coefficients are experimental values at these positions.

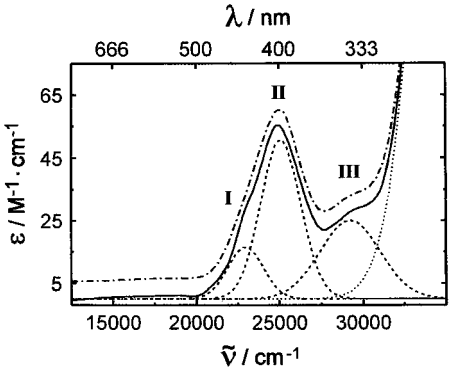

Figure 10. Electronic spectrum of **5a** (—) in CH_3CN and its deconvolution (- - -) with three absorption maxima I–III of Gaussian line shape. The resulting calculated spectrum (— · —) is offset by 5 M^{-1} cm^{-1} for the sake of clarity.

weakened (or canceled) in **4b** where the Cr–N_α–N_β bond angle deviates significantly from linearity. Note that the Cr–N_α bond distance in **4a** at 2.322(5) Å is slightly (barely significantly) shorter than in **4b** at 2.350(3) Å; i.e., this bond is slightly less covalent in **4b** than in **4a**.

Electronic Spectra of Nitridochromium(V) Complexes. The electronic spectra of new nitridochromium(V) complexes have been recorded in acetonitrile solution at ambient temperature in the range 200–1600 nm. The results are summarized in Table 4.

Figure 10 shows the spectrum of the mononuclear species **5a**. In the range 450–350 nm a broad, unsymmetrical absorption maximum of low intensity ($\epsilon < 55$ M^{-1} cm^{-1}) is observed which is accompanied by a shoulder at ~330 nm ($\epsilon \sim 25$ M^{-1} cm^{-1}). This spectrum can be readily deconvoluted by a fit to three absorption maxima of Gaussian line shape, respectively. Identical patterns have been obtained for **3b** and **4a**. Thus the electronic spectra of complexes containing the $[Cr^V(N)(cyclam)]^{2+}$ fragment each display three low-intensity d–d transitions at ~430 nm (band I), ~400 nm (band II), and ~350 nm (band III). In the spectra of **3b** and **4a** an $N_3^- \rightarrow Cr^V$ ligand-to-metal charge transfer (CT) band of medium intensity at ~305 nm ($\epsilon \sim 500$ M^{-1} cm^{-1}) and an $N_3^-(\pi \rightarrow \pi^*)$ CT band at ~260 nm of large intensity ($\epsilon > 3 \times 10^3$ M^{-1} cm^{-1}) are observed.

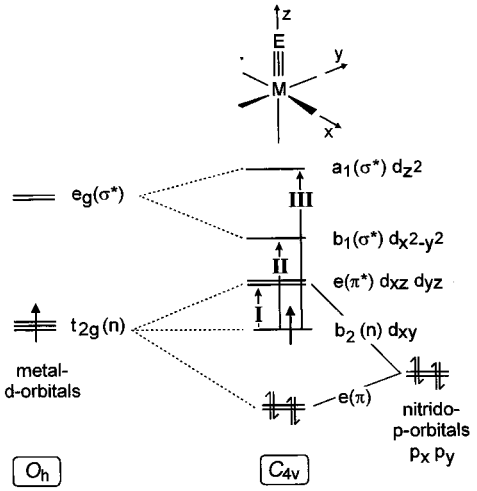

Figure 11. Molecular orbital diagram for a C_{4v} metal–nitrido complex according to ref 13.

The assignment of bands I–III is unambiguously achieved by following the Ballhausen–Gray ligand-field model[13] for $[V(O)(OH_2)_5]^{2+}$ as shown schematically in Figure 11. To a first approximation the present $[Cr^V(N)(cyclam)Y]^{n+}$ complexes possess a N≡Cr^VN_5 first coordination sphere of C_{4v} symmetry. Due to the strong π-donating nitrido ligand the degenerate t_{2g} orbitals (in O_h symmetry) split into a nonbonding $b_2(xy)$ and two degenerate antibonding, e(xz,yz), d orbitals and the—in O_h symmetry degenerate—antibonding e_g* orbitals split into antibonding $b_1(x^2 - y^2)$ and $a_1(z^2)$ orbitals. The energeticially lowest transition (band I) is then assigned to the symmetry-allowed $^2B_2 \rightarrow {}^2E$ transition, $(xy) \rightarrow (xz,yz)$. Band II corresponds to the $^2B_2 \rightarrow {}^2B_1$, $(xy) \rightarrow (x^2 - y^2)$, transition, whereas band III is a $^2B_2 \rightarrow {}^2A_1$, $(xy) \rightarrow (z^2)$, transition.

With these assignments of the d–d transitions and their corresponding energies as well as the structural parameters of the $[Cr^V(N)(cyclam)Y]^{n+}$ species it is possible to directly calculate the energies of the following parameters of the angular-overlap model (AOM): e_σ^{ax}, e_π^{ax}, e_σ^{cyclam}. Two simple assumptions are made: (i) The ligand cyclam is a pure σ-donor and described by a single parameter e_σ^{cyclam}, and (ii) the bond angle N≡Cr–Y is 180°. The latter has the consequence that the AOM parameters for the nitride and the ligand Y in trans position located on the molecular z-axis are described by two parameters only, namely e_σ^{ax} and e_π^{ax}. This model represents a completely general ligand-field model which includes rigorous treatment of spin–orbit coupling. The admixing of ligand and metal orbitals is not explicitly modeled, but covalency has parametric consequences. With these assumptions the parameter space is 4-dimensional for d^1 systems.

(13) (a) Ballhausen, C. J.; Gray, H. B. *Inorg. Chem.* **1962**, *1*, 111. (b) Winkler, J. R.; Gray, H. B. *J. Am. Chem. Soc.* **1983**, *105*, 1373. (c) Winkler, J. R.; Gray, H. B. *Inorg. Chem.* **1985**, *24*, 346. (d) Miskowski, V. M.; Gray, H. B.; Hopkins, M. D. in *Advances in Transition Metal Coordination Chemistry*; Che, C.-M., Yam, V. W. W., Eds.; JAI Press Inc.: Greenwich, London, **1996**; Vol 1, pp 159–186.

As a result, we have obtained the following energies: $e_\sigma^{ax} = 22\,000\ cm^{-1}$; $e_\pi^{ax} = 21\,300-25\,000\ cm^{-1}$; $e_\sigma^{cyclam} = 7300-8600\ cm^{-1}$.

From the electric dipole transitions $^2B_2 \rightarrow {}^2E(I)$ and $^2B_2 \rightarrow {}^2B_1(II)$ and the $g_\perp$ and $g_\parallel$ values from EPR spectroscopy the spin−orbit coupling constant ζ_{3d} can be calculated by using eqs 5 and 6.

$$g_\perp = g_e\left(1 - \frac{\zeta}{\Delta_1(^2E - {}^2B_2)}\right) \quad (5)$$

$$g_\parallel = g_e\left(1 - \frac{4\zeta}{\Delta_2(^2B_1 - {}^2B_2)}\right) \quad (6)$$

A small value for ζ_{3d} of $\sim 88\ cm^{-1}$ is obtained. This value is in excellent agreement with $\zeta_{3d} = 75\ cm^{-1}$ reported by Gray et al.[14] for $Rb_2[Cr^V(O)Cl_5]$ ($\Delta_1 = 12\,900\ cm^{-1}$, $\Delta_2 = 23\,500\ cm^{-1}$; $\langle g \rangle = 1.986$) and is reduced by 75% in comparison with the value reported for a gaseous Cr^V ion ($\zeta_{3d} = 380\ cm^{-1}$).[15]

The e_σ^{cyclam} value is reasonably established by the electronic spectra of *trans*-$[Cr^{III}Cl_2(cyclam)]^+$ and **2a** to be in the range 6600−6900 cm^{-1}. This represents a lower limit for Cr^V(cyclam) since one expects an increase of a σ-donor parameter on going from Cr(III) to Cr(V). On the other hand, the $Cr-N_{cyclam}$ bond distances in **2a** and the *trans*-$[Cr^V(N)(cyclam)]^{2+}$ species are very similar which implies that the e_σ^{cyclam} values should not be too different. Thus a value of 7300 cm^{-1} is very reasonable.

Ligand-field parameters for the nitrido ligand are scarce. For $[Os(N)Cl_4]^-$ Gray et al.[16] find $E(e) - E(b_2)$, which in our parametrization is equal to e_π^{ax}, to be 36 000 cm^{-1} whereas $E(a_1) - E(b_2)$, which represents $2e_\sigma^{ax} - e_\sigma^{cyclam}$ here, was estimated to be 49 000 cm^{-1}. If one takes into account that ligand-field splittings are approximately twice as large for complexes of the third transition metal series as for analogous complexes of the first period, we arrive at estimates for e_π^{ax} and e_σ^{ax} around 18 000 and 25 000 cm^{-1}, respectively. The calculated values are in this ballpark. In fact, in a similar analysis for the corresponding $[Mn^V(N)(cyclam)Y]^{n+}$ complexes,[17] we report e_σ^{ax} to be 27 200 cm^{-1}, $e_\pi^{ax} = 18\,800\ cm^{-1}$, and $e_\sigma^{cyclam} = 7340\ cm^{-1}$.

From the determined parameters the corresponding one-electron energies are calculated straightforwardly by using the information given in Figure 12. The splitting pattern is best described as 1 + 3 + 1 rather than the traditional 1 + 2 + 1 + 1 Ballhausen−Gray pattern for $[OV(OH_2)_5]^{2+}$. This is in line with recent results of Fujii et al.[18] on five-coordinate oxo- and nitridochromium(V) porphinato complexes with the Cr(V) center 0.5 Å above the plane of the auxiliary porphinate. For these systems the authors have shown that the $d_{x^2-y^2}$ orbital is *lower* in energy than the degenerate set of d_{xy},d_{xz} orbitals. It is gratifying that the six-coordinate $[(cyclam)Cr^V(N)Y]^{n+}$ complexes with the metal ion only 0.25 Å above the plane of amine nitrogens fits between this model and the traditional Ballhausen−Gray scheme.

Conclusion

By using spectroscopically innocent (i.e. in the visible transparent) auxiliary amine ligands such as cyclam, it has been possible to fully characterize for the first time the electronic structure of d^1 electron configurated nitridochromium(V) complexes. Three low-intensity (ϵ < 100 L mol^{-1} cm^{-1}) d−d transitions are observable at ∼430, ∼400, and ∼350 nm which are assigned to $^2B_2 \rightarrow {}^2E$, $^2B_2 \rightarrow {}^2B_1$, and $2B_2 \rightarrow {}^2A_1$ transitions in C_{4v} symmetry, respectively.

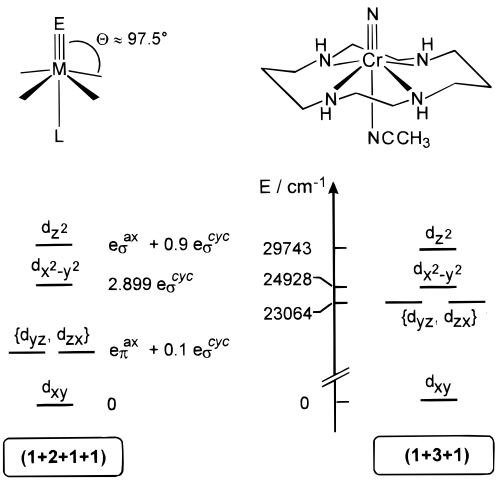

Figure 12. Orbital splitting diagram for axial systems with a single strong π-donor ligand ($E = O^{2-}$, N^{3-}) and calculated orbital energies for **5a** using the following parameters: $e_\sigma^{ax} = 22\,000$, $e_\pi^{ax} = 22\,200$, $e_\sigma^{cyclam} = 8600\ cm^{-1}$, and $\theta = 97.5°$.

Experimental Section

The starting materials *cis*- and *trans*-$[Cr^{III}(cyclam)Cl_2]Cl$ were prepared according to published procedures.[11,19]

Caution! *Although we have encountered no problems in the present study, it is stressed that perchlorate salts are potentially explosive.*

Preparation of Complexes. *Small amounts only should be prepared and handled with appropriate precautions.*

***cis*-[Cr^{III}(cyclam)(N$_3$)$_2$](ClO$_4$) (1a).** A mixture of *cis*-$[Cr(cyclam)Cl_2]Cl$ (0.50 g; 1.40 mmol) and NaN_3 (1.8 g; 28 mmol) in dry ethanol was heated to reflux for 24 h during which time a red microcrystalline precipitate formed which was filtered off. Recrystallization of this material from an acetonitrile/water mixture (5:1 vol) with addition of 0.1 M aqueous perchloric acid produced within a few days at 4 °C red crystals of **1a** suitable for X-ray crystallography. Yield: 0.35 g (57%). IR (KBr disk), cm^{-1}: $\nu(N_3)$, 2085 (vs), 2058 (vs); $\gamma(N-H)$, $\delta(CH_2)$, 865, 851, 808, 800. μ(30−300 K), μ_B: 3.85. Anal. Calcd for $C_{10}H_{24}N_{10}CrClO_4$: C, 27.06; H, 5.92; N, 31.71. Found: C, 27.3; H, 5.7; N, 32.0.

***trans*-[Cr^{III}(cyclam)(N$_3$)$_2$](ClO$_4$) (2a).** Addition of a saturated aqueous $NaClO_4$ solution to the above red filtrate initiated the precipitation of red crystals of **2a** in 40% yield (0.24 g). Similarly, addition of solid $NaBPh_4$ (1.0 g) to the above ethanol solution yields red crystals of the tetraphenylborate salt **2b**. IR (KBr disk), cm^{-1}: $\nu(N_3)$, 2085 (vs), 2069 (vw); $\gamma(N-H)$, $\delta(CH_2)$, 880, 802. μ(30−300 K), μ_B: 3.77. Anal. Calcd for $C_{10}H_{24}N_{10}CrClO_4$: C, 27.06; H, 5.92; N, 31.71. Found: C, 26.9; H, 5.8; N, 31.5.

***trans*-[Cr^V(N)(cyclam)(N$_3$)]X (X = ClO$_4$ (3a), BPh$_4$ (3b)).** Finely ground red **2a** or **2b** (0.5 g) was thinly dispersed over an aluminum foil and irradiated with a 300 W lamp until the red color of the starting material had changed to bright yellow. The yield of **3a** or **3b** is quantitative. Data for **3b** are as follows. IR (KBr disk), cm^{-1}: $\nu(N_3)$, 2076, 2055, 2036, 2022; $\gamma(N-H)$, $\delta(CH_2)$, 880, 801; $\nu(Cr{\equiv}N)$, 967. Anal. Calcd for $C_{34}H_{44}N_8CrB$ (**3b**): C, 65.07; H, 7.07; N, 17.85. Found: C, 65.2; H, 7.0; N, 17.7.

(14) Gray, H. B.; Bernal, I.; Hare, C. R. *Inorg. Chem.* **1962**, *1*, 831.
(15) Bendix, J.; Brorson, M.; Schäffer, C. E. *Inorg. Chem.* **1993**, *32*, 2838.
(16) Cowman, C. D.; Trogler, W. C.; Mann, K. R.; Poon, C. K.; Gray, H. B. *Inorg. Chem.* **1976**, *15*, 1747.
(17) Meyer, K.; Bendix, J.; Metzler-Nolte, N.; Weyhermüller, T.; Wieghardt, K. *J. Am. Chem. Soc.* **1998**, *120*, 7260.
(18) Fujii, H.; Yoshimura, T.; Kamada, H. *Inorg. Chem.* **1997**, *36*, 1122.
(19) (a) Flores-Velez, L. M.; Sosa-Rivadeneyra, J.; Sosa-Torres, M. E.; Rosales-Hoz, M. J.; Toscano, R. A. *J. Chem. Soc., Dalton Trans* **1991**, 3243. (b) Sosa, M. E.; Tobe, M. L. *J. Chem. Soc., Dalton Trans* **1986**, 427.

Table 5. Crystallographic Data for **1a**, **2b**, **4a**·3.5H_2O, **4b**·2EtOH, **5a**, and **5b**·MeCN·H_2O

	1a	**2b**	**4a**·3.5H_2O	**4b**·2EtOH	**5a**	**5b**·MeCN·H_2O
chem formula	$C_{10}H_{24}N_{10}ClCrO_4$	$C_{34}H_{44}BCrN_{10}$	$C_{20}H_{55}Cl_3Cr_2N_{13}O_{15.5}$	$C_{72}H_{100}B_2Cr_2N_{16}O_2$	$C_{12}H_{27}Cl_2CrN_6O_8$	$C_{62}H_{72}B_2CrN_7O$
fw	435.84	655.60	936.12	1347.30	506.30	1004.89
space group	$P2_1/c$	*Pbca*	*Pnma*	$C2/c$	$P2_1/n$	$P\bar{1}$
a, Å	13.636(3)	10.228(1)	16.797(2)	22.834(3)	10.812(2)	11.951(1)
b, Å	8.754(2)	21.588(2)	25.132(3)	17.803(2)	12.871(2)	12.875(2)
c, Å	15.249(3)	29.222(3)	18.783(2)	18.163(2)	15.348(3)	17.897(2)
α, deg	90	90	90	90	90	84.71(2)
β, deg	100.36(3)	90	90	97.07(2)	103.46(2)	84.52(2)
γ, deg	90	90	90	90	90	88.67(2)
V, Å	1790.6(7)	6452.3(11)	7929(2)	7327(2)	2077.1(6)	2729.4(8)
Z	4	8	8	4	4	2
T, K	100(2)	103(2)	173(2)	100(2)	100(2)	173(2)
ρ_{calcd}, g cm^{-3}	1.617	1.350	1.568	1.221	1.619	1.223
no. of data	4263	13 870	37 990	16 010	8956	12 529
no. of unique data	3723	4577	8190	5634	3439	9110
no. of params	235	415	507	435	263	660
μ(Mo Kα), cm^{-1}	8.30	3.97	8.29	3.52	8.60	2.58
R1[a]	0.0612	0.0675	0.0768	0.0566	0.0471	0.0564
wR2[b] (all data)	0.1974	0.1644	0.2171	0.1938	0.1254	0.1523

[a] Observation criterion: $I > 2\sigma(I)$. $R1 = \Sigma||F_o| - |F_c||/\Sigma|F_o|$. [b] $wR2 = [\Sigma[w(F_o^2 - F_c^2)^2]/\Sigma[w(F_o^2)^2]]^{1/2}$, where $w = 1/\sigma^2(F_o^2) + (aP)^2 + bP$ and $P = (F_o^2 + 2F_c^2)/3$.

[{*trans*-[Cr^V(N)(cyclam)]}$_2$(μ-N_3)](ClO$_4$)$_3$·3.5H_2O (4a). The complex **4a** was obtained by crystallization of **3a** from aqueous solution by addition of $NaClO_4$·H_2O or, alternatively, by photolysis of an aqueous solution of **1a** or **2a**. The details of the latter process are now described. An argon-purged aqueous solution or suspension (100 mL) of **1a** or **2a** (1.0 g; 2.29 mmol) was irradiated at ambient temperature with external water cooling with a Hg immersion lamp (Osram HPK 200) for 45 min. A constant stream of argon gas was passed through the solution/suspension during irradiation. A clear bright yellow solution was obtained from which upon slow evaporation of the solvent yellow hexagonal crystals of **4a** precipitated within a few days. Yield: 0.96 g (90%). IR (KBr disk), cm^{-1}: $\nu(N_3)$, 2108 (vs), 2036 (m); γ(N−H), $\delta(CH_2)$, 882, 808; ν(Cr≡N), 986. Anal. Calcd for $C_{20}H_{55}N_{13}Cr_2Cl_3O_{15.5}$: C, 25.66; H, 5.92; N, 19.45. Found: C, 25.9; H, 5.7; N, 19.4.

Yellow crystals of [{*trans*-[Cr^V(N)(cyclam)]}$_2$(μ-N_3)](BPh$_4$)$_2$(N_3)·2C_2H_5OH (**4b**) were grown by recrystallization of **3b** from an ethanol/acetone (1:1) mixture. IR (KBr disk), cm^{-1}: $\nu(N_3)$, 2096−2028 (vs, b); γ(N−H), $\delta(CH_2)$, 880, 800; ν(Cr≡N), 976. Anal. Calcd for $C_{72}H_{100}N_{16}Cr_2B_2O_2$: C, 64.18; H, 7.48; N, 16.63. Found: C, 64.0; H, 7.3; N, 16.6.

***trans*-[Cr^V(N)(cylam)(NCCH$_3$)]X_2 (X = ClO$_4$ (5a), BPh$_4$ (5b)).** To a suspension of **4a** (0.50 g; 0.53 mmol) in acetonitrile (25 mL) was added solid $AgClO_4$ (0.11 g; 0.53 mmol) with stirring. Upon gentle warming of this suspension a voluminous precipitate of AgN_3 formed which was carefully filtered off (caution: *AgN_3 is explosive and should not be dried but immediately dissolved in aqueous NH_3*). To the clear yellow solution dry ethanol (25 mL) was added which initiated the precipitation of microcrystalline **5a** within 12 h at 4 °C. Recrystallization of this material from acetonitrile/toluene mixture (1:1) yielded crystals suitable for X-ray crystallography. Single crystals of the tetraphenylborate salt *trans*-[Cr^V(N)(cyclam)(NCCH$_3$)](BPh$_4$)$_2$·CH_3CN·H_2O (**5b**) were obtained from an acetonitrile solution of **5a** by addition of $NaBPh_4$. Yield (**5a**): 0.46 g (85%). IR (KBr disk), cm^{-1} of **5a**: ν(Cr≡N), 996; γ(N−H), $\delta(CH_2)$, 878, 808. Raman spectrum **5a**, cm^{-1}: ν(C≡N), 2261; ν(Cr≡N), 995. Anal. Calcd for $C_{12}H_{27}N_6CrCl_2O_8$: C, 28.47; H, 5.37; N, 16.60. Found: C, 28.6; H, 5.3; N, 16.8.

Physical Measurements. Electronic spectra were recorded on an Perkin-Elmer Lambda 19 (range: 200−1600 nm) spectrophotometer; infrared and Raman (λ = 1064 nm) spectra, on solid samples (KBr disks) on a Perkin-Elmer 2000 FT-IR/FT-NIR Raman spectrometer. The X-band EPR spectra of the complexes were recorded on a Bruker ESP 300E spectrometer equipped with an Oxford Instruments ESR 910 helium-flow cryostat. Simulations of the spectra were performed by using the Simfonia program (Bruker). Temperature-dependent magnetic susceptibilities of powdered samples were measured by using a SQUID magnetometer (Quantum Design) at 1.0 and 0.1 T (4.2−300 K).

X-ray Crystallographic Data Collection and Refinement of the Structures. Red single crystals of **1a** and **2b** and yellow crystals of **4a**,**b** and **5a**,**b** were mounted in sealed glass capillaries. Graphite-monochromated Mo Kα radiation (λ = 0.710 73 Å) was used throughout. Crystallographic data for the compounds are listed in Table 5. Cell constants for **1a** were obtained from a least-squares fit of the setting angles of 25 carefully centered reflections. Intensity data for this compound were collected on an Enraf-Nonius CAD4 diffractometer using the $\omega-2\theta$ scan technique. Data were corrected for Lorentz and polarization effects, but no absorption correction was carried out due to a small absorption coefficient. Compounds **2b**, **4a**,**b**, and **5a**,**b** were measured on a Siemens SMART CCD-detector system equipped with a cryogenic nitrogen cold stream. Cell constants were obtained from a subset of at least 6000 stronger reflections. Data collection was performed by a hemisphere run taking frames at 0.30° in ω. Corrections for Lorentz and polarization effects and a semiempirical absorption correction using the program SADABS[20] were applied. The Siemens ShelXTL[21] software package was used for solution, refinement, and artwork of the structures. All structures were solved and refined by direct methods and difference Fourier techniques performed on DEC Alpha workstations. Neutral atom scattering factors were obtained from tables.[22] All non-hydrogen atoms were refined anisotropically except those of disordered parts of a perchlorate anion in **4a** and solvent molecules in **4a**,**b**, which were isotropically refined by split atom models. All hydrogen atoms were placed at calculated positions and refined as riding atoms with isotropic displacement parameters. C atoms in **4a** were found to have large anisotropic thermal components along the C−C and C−N bonds in the macrocycle. This is due to the crystallographically imposed mirror plane bisecting the cation which in fact has a slightly lower symmetry. Details are given in the Supporting Information.

Acknowledgment. J.B. thanks the University of Copenhagen (Chemistry Department) for granting a leave of absence. Financial support of this work from the Fonds der Chemischen Industrie is also gratefully acknowledged.

Supporting Information Available: Tables of crystallographic and structure refinement data, atom coordinates and U_{eq} values, bond lengths and angles, anisotropic thermal parameters, and calculated and refined positional parameters of hydrogen atoms for the complexes (40 pages). Ordering information is given on any current masthead page.

IC980302Q

(20) Sheldrick, G. M. Universität Göttingen, 1994.
(21) *ShelXTL V. 5*; Siemens Analytical X-ray Instruments, Inc.: Madison, WI, 1994.
(22) *International Tables for X-ray Crystallography;* Kynoch Press: Birmingham, U.K., 1991.